Flame Propagation in Nano-metal Dust Explosions

GAO, Wei[1], BI, Mingshu[1], MOGI, Toshio[2], DOBASHI, Ritsu[2]
[1] School of Chemical Machinery and Safety Engineering, Dalian University of Technology
Dalian, Liaoning 116024, China
[2] Department of Chemical System Engineering, School of Engineering, The University of Tokyo
Hongo 7-3-1, Bunkyo-ku, Tokyo 113-8656, Japan

1 Introduction

To take appropriate measures preventing accidental dust explosions, it is necessary to sufficiently understand the flame propagation mechanisms in this phenomenon. As yet no unified theory exists covering the entire flame process from pre-flame reaction to the final state of the combustion products due to two major problems facing flame propagation research in dust explosions [1, 2]. One is the complexity of the particle cloud of the combustion processes. During dust flame propagation, the flame propagates in the region where combustible particles and vaporized gas and/or liquefied particles coexist. In addition, the flame propagation process is always unsteady and numerous factors govern the initiation and subsequent propagation of the dust flames, such as the physical and chemical properties of the fuel, the average size, shape, concentration and distribution of the particles, moisture, oxygen concentration, the initial pressure, and the initial turbulence intensity.

Flame propagation behaviors, combustion reaction states and products of 40 nm titanium, aluminium and iron particles in dust explosions were compared to reveal the effects of metal properties on dust explosion mechanism.

2 Experimental apparatus and materials

The open-space dust explosion experimental apparatus shown in Figure 1 was used in this study. It consisted of combustion tubes, a dispersion system, a gas supplying system, an ignition system, a high-speed photography system and a time controller system.

40 nm aluminium, titanium and iron particles were chosen as the experimental samples. The properties of aluminium, titanium and iron metals are listed in table 1. Particle size distributions were measured by Malvern Nano-ZS90 laser particle size analyser. The z-average diameters of 40 nm aluminium, titanium and iron particles were 510.3 nm, 514.9 nm, and 3358 nm, respectively. These results indicated that

Correspondence to: gaoweidlut@dlut.edu.cn

agglomeration effects existed in the three experimental samples, and were most serious in 40 nm iron particles due to its important magnetic properties and larger density.

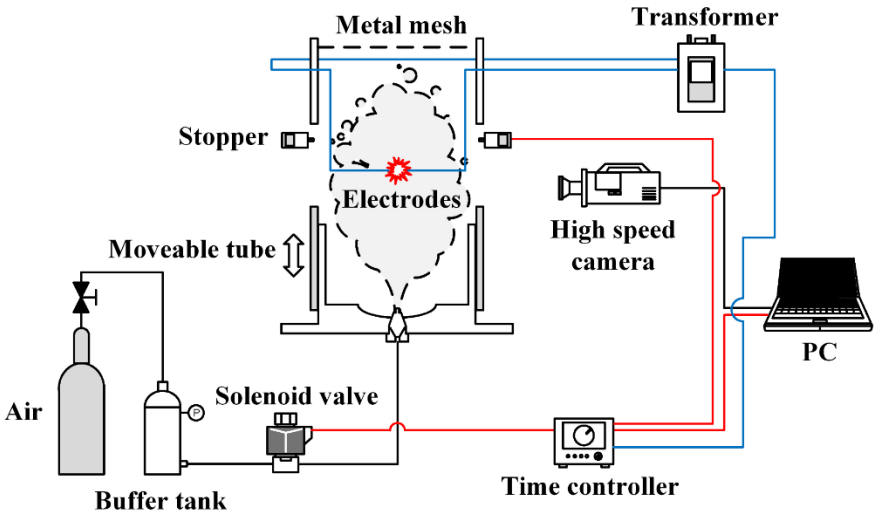

Figure 1 Experimental apparatus

Table 1: Properties of aluminium, titanium and iron particles

Symbol	Al	Ti	Fe
Standard state (298 K)	Solid	Solid	Solid
Relative atomic mass	26.982	47.867	55.845
Density of solid [kg/m^3]	2700	4507	7874
Melting point [K]	933.47	1941	1811
Boiling point [K]	2792	3560	3134
Enthalpy of fusion [kJ/mol]	10.7	18.7	13.8
Enthalpy of vaporization [kJ/mol]	293	425	347
Thermal conductivity [W/m/k]	235	21.9	80

3 Results and discussion

3.1 Flame propagation behaviors and velocities

Flame propagations in 40 nm titanium, aluminium and iron dust clouds are shown in Figure 2. The nominal dust concentrations were 1000 g/m^3. It could be observed that 40 nm titanium, aluminium and iron dust flames were all developed as approximately spherical flame and characterized by discrete single glowing burning particles that uniformly distributed in the combustion zone. 40 nm titanium dust flame developed very quickly. 100 ms after ignition the flame already propagated to the top of the open combustion space. Whereas for 40 nm aluminium dust flame, after 180 ms the flame still did not propagate to the top. 40 nm iron dust flame propagated most slowly. All these results indicated that 40 nm titanium dust cloud was more easily to be ignited and propagated due to its high combustion enthalpy and reactive characteristic that burned not only with oxygen in air, but also with nitrogen. In the flame propagations, the smaller particles

in the flame front were first participated in the combustion reaction. The larger unburnt particles around absorbed the released heat through thermal convection and thermal radiation emitted from the burning particles, and reacted with oxygen or nitrogen.

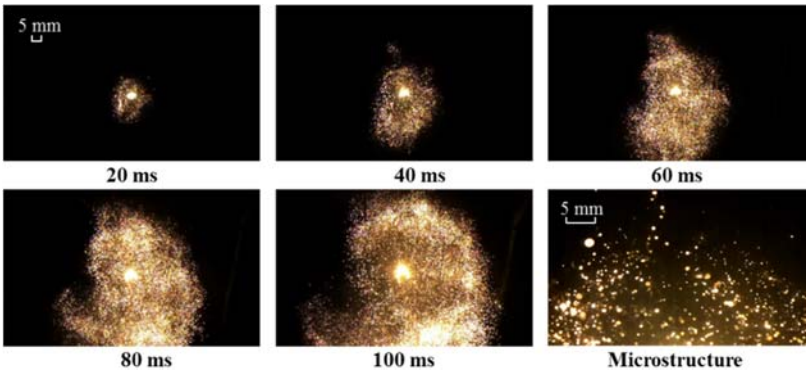

(a) Flame propagation in titanium dust cloud

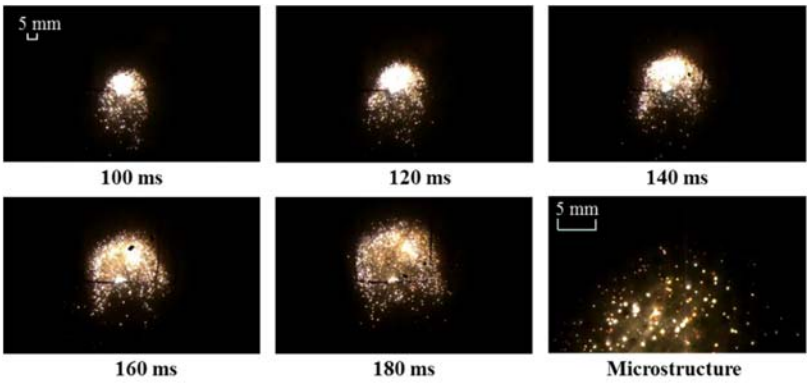

(b) Flame propagation in aluminium dust cloud

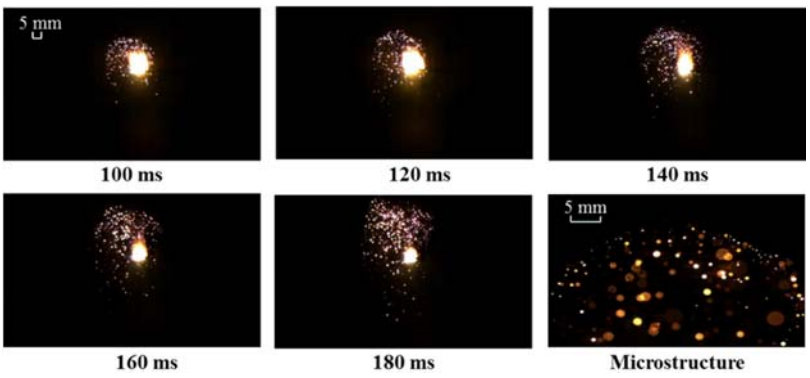

(c) Flame propagation in iron dust cloud

Figure 2 Flame propagations in Nano-metal dust clouds

Pulsating flame propagation shown in Figure 3 appeared in the Nano-metal dust explosions. 40 nm titanium dust flame pulsated most seriously with the average velocity of 0.565 m/s. 40 nm iron dust flame pulsated least seriously with the average velocity of 0.035 m/s. 40 nm aluminium dust flame pulsated with the average velocity of 0.189 m/s. As for 40 nm iron dust particles, the density was the largest among the three samples and the particle agglomerates were most serious, which meant that the downward sedimentation effect could not be neglected. The smallest density and lowest melting and boiling point of 40 nm aluminium particles would lead to the faster flame propagation velocity compared with 40 nm iron particles. When flame propagation velocity was rapid, there was insufficient time for the particles to be heated by radiation or convection from the burned region. As a result the velocity was slowed down because the heat was absorbed by cold particles in front of the flame front. However, when the velocity was slow, the particles in front of the flame were sufficiently heated by radiation or convection from the hot particles behind the flame so that the flame gathered speed. After passing through this period, the flame met the cold particles, and its speed was again decreased. Dust stratification caused by the velocity difference between particles and ambient gases was the second reason for the pulsating flame propagation. Residual turbulence in the dust cloud caused by dispersion and turbulence produced by thermal expansion of combustion products were also contributed to the flame pulsation in propagation.

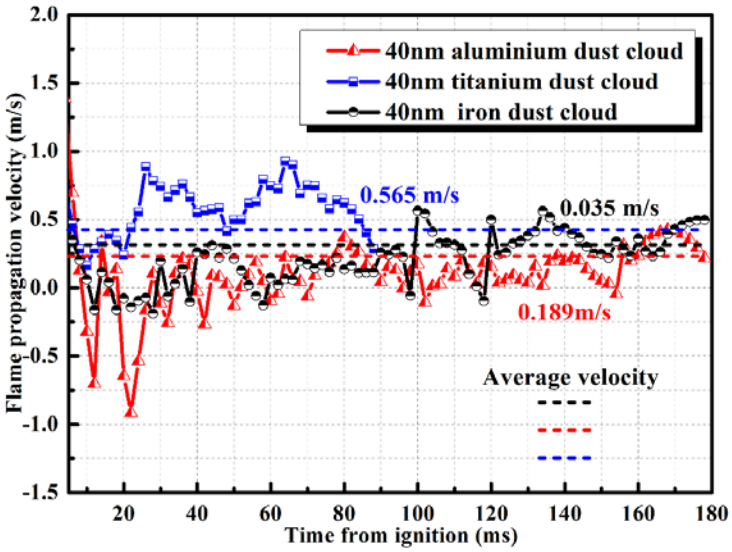

Figure 3 Flame propagation velocities in Nano-metal dust clouds

3.2 Combustion products analysis

The unburnt metal particles and combustion products of 40 nm titanium, aluminium and iron were visualized by the scanning electron microscope (SEM) and transmission electron microscope (TEM). From the SEM photographs shown in Figure 4, it was observed that unburnt 40 nm titanium particles were in approximately spherical shape with serious agglomeration effect. However, the combustion products exhibited complicated structures combined the spherical titanium oxides with considerable larger diameters and irregularly spliced smaller titanium oxides that probably formed after “micro explosion” in burning process. It was illustrated that the amount of 40 nm titanium reacted through gas phase reactions was insignificant. The combustion reaction of 40 nm titanium might occur in liquid-phase. As for 40 nm aluminium particles, the unburnt particles presented regular spherical shape with observably agglomerates in larger size and irregular shape.

Whereas the irregular spliced shapes of 40 nm aluminium combustion products once proved that they were formed by condensations of gas-phase reaction. Due to the important magnetic properties of 40 nm iron particles, TEM was used to observe the particles. The unburnt particles were in spherical shape with agglomeration effect. After explosion the products were still in spherical shape with larger size, which indicated that the combustion of 40 nm iron were in solid-phase surface oxidation.

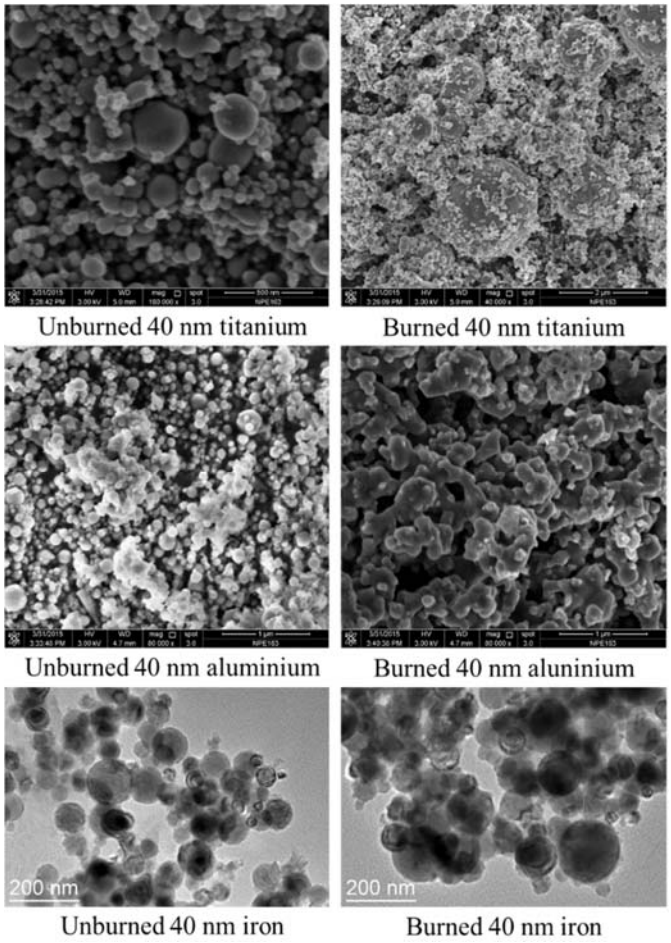

Figure 4 SEM and TEM photographs of Nano-metal particles

To specify the chemical composition of the combustion products, X-ray photoelectron spectroscopy (XPS) was performed using an ESCALAB250 XPS system with a non-monochromated Al Kα X-ray source at 1486.6 eV. Ti2p spectrum was resolved into four pair spin-orbit contributions at binding energies $E_b(Ti2p_{3/2})$ of 458.141 eV, 456.964 eV, 454.398 eV and 455.8 eV, which were assigned to the binging energy of Ti in TiO_2 (Ti^{4+}), Ti_2O_3(Ti^{3+}), TiO (Ti^{2+}) and TiN (Ti^{3+}), respectively. Al2p high resolution spectrum illustrated that 40 nm aluminium combustion products only contained Al_2O_3 (Al^{+3}) at the binding energy $E_b(Al2p_{3/2})$ of 74.104 eV. Fe2p high resolution spectrum indicated that 40 nm iron combustion products consisted of Fe_2O_3 (Fe^{3+}), Fe_3O_4 (Fe^{3+}/Fe^{2+}) and FeO (Fe^{2+}) corresponding to the binding energies $E_b(Fe2p_{3/2})$ of 712.425 eV, 710.747 eV and 709.683 eV, respectively. The results are shown in Table 2.

Table 2: Peak fitting parameters of the high resolution spectra of the Ti2p region for 40 nm titanium combustion products, Al2p region for 40 nm aluminium combustion products and Fe2p region for 40 nm iron combustion products

Combustion Products	$E_b(Ti2p_{3/2})$/ eV	$E_b(Al2p_{3/2})$/ eV	$E_b(Fe2p_{3/2})$/ eV	$A_i/\Sigma A_i$/ %	FWHM/ eV	Valence of metal
40 nm titanium	458.141	--	--	43	1.496	Ti^{4+} (TiO_2)
	456.964	--	--	27	2.483	Ti^{3+} (Ti_2O_3)
	454.398	--	--	21	1.716	Ti^{2+} (TiO)
	455.8	--	--	9	1.68	Ti^{3+} (TiN)
40 nm aluminium	--	74.104	--	100	2.616	Al^{3+} (Al_2O_3)
40 nm iron	--	--	712.425	49	3.682	Fe^{3+} (Fe_2O_3)
	--	--	710.747	26	2.215	Fe^{3+}/ Fe^{2+} (Fe_3O_4)
	--	--	709.683	15	1.897	Fe^{2+} (FeO)
	--	--	719.158	10	3.46	Fe(Ⅲ)

Results showed that 40 nm titanium combustion products contained 43% TiO_2 (Ti^{4+}), 27% Ti_2O_3 (Ti^{3+}), 21% TiO (Ti^{2+}) and 9% TiN (Ti^{3+}), 40 nm aluminium combustion products contained 100% Al_2O_3 (Al^{3+}), and 40 nm iron combustion products contained 49% Fe_2O_3 (Fe^{3+}), 26% Fe_3O_4 (Fe^{3+}/Fe^{2+}), 15% FeO (Fe^{2+}) and 10% nonoxides Fe(Ⅲ). Inerted by nitrogen for preventing nano-titanium dust explosions was inadvisable.

4 Conclusions

To reveal the effects of metal properties on dust explosion mechanism, experiments were conducted to examine the flame propagation behaviors, combustion reaction states and products of 40 nm titanium, aluminium and iron particles in dust explosions. The conclusions obtained were as follows:

(1) 40 nm titanium, aluminium and iron dust flames were all developed in approximately spherical shape and characterized by discrete single glowing burning particles uniformly distributed in the combustion zone. The average pulsating flame propagation velocities in 40 nm titanium, aluminium and iron dust clouds were 0.565 m/s, 0.189 m/s and 0.035 m/s, respectively.

(2) Combustion reaction occurred in liquid-phase for 40 nm titanium particles, gas-phase for 40 nm aluminium particles, and solid-phase for 40 nm iron particles. 40 nm titanium combustion products contained 43% TiO_2 (Ti^{4+}), 27% Ti_2O_3 (Ti^{3+}), 21% TiO (Ti^{2+}) and 9% TiN (Ti^{3+}). 40 nm aluminium combustion products contained 100% Al_2O_3 (Al^{3+}). 40 nm iron combustion products contained 49% Fe_2O_3 (Fe^{3+}), 26% Fe_3O_4 (Fe^{3+}/Fe^{2+}), 15% FeO (Fe^{2+}). Inerted by nitrogen for preventing nano-titanium dust explosions was inadvisable.

References

[1] Eckhoff R. K. (2003). Dust explosions in the process industries. Gulf Professional Publishing. 4: 251

[2] Palmer K.N. (1973). Dust Explosions and Fires. Chapman and Hall. 2: 23